First-principles study of electronic, magnetic and optical properties of Zr_2NiB full-Heusler compound

Student ID: 171322
Session: 2017-2018

Report submitted to the Department of Physics at
Jashore University of Science and Technology
in partial fulfillment of the requirements
for the degree of Bachelor of Science
with Honours in Physics

December 2022

Abstract

The electronic, magnetic and optical properties of Zr based full-Heusler alloy Zr_2NiB was studied using the spin-polarized full-potential linearized augmented plane wave (FP-LAPW) method based on density functional theory (DFT). The optimized lattice parameter was estimated to be 6.266 Å. Our study revel that for the alloy, both the spin up and spin down states are conducting, demonstrating the alloy to be in metallic nature. The total magnetic moment of this alloy is 0.99 μ_B, indicating the alloy is ferromagnetic. Optical properties such as dielectric function, reflectivity, refractivity, absorption coefficient, optical conductivity were also calculated.

Acknowledgements

Firstly, I praise and thank almighty Allah, the Lord of the worlds, the Most Merciful, the Guider of hearts, the Provider of sustenance, the Owner of life and death.

I would like to thank my respected supervisor, Dr. Mohammad Abdur Rashid, for his continuous supervision and constant guidance to complete my project work properly. During the period of this project, he always shows me invaluable confidence.

I am also grateful to the writers of several articles (included in the bibliography), from where I have gleaned a wealth of additional data. I would like to thank my group members who helped me a lot.

I would never forget to pay thanks to my parents from the core of my heart for their love, unconditional supporting and prayers in all steps in my life. Their love and encouragement always gives me mental support to continue my study smoothly.

Contents

List of Figures

List of Tables

First-principles study of electronic, magnetic and optical properties of Zr_2NiB full-Heusler compound

Chapter 1

Introduction

Heusler alloys have garnered more attention in recent years due to their intriguing physical features [1–4], particularly the half-metallic (HM) character, which was first predicted by de Groot et al in 1983 [5], whose majority-spin band is metalic while the minority-spin band is semiconducting with an energy gap at the Fermi level (E_F), HM ferromagnets have received great attention from scientific researchers due to potential applications in spintronic devices, such as the magnetic sensor, the tunnel junction, the spin valve as well as the primary materials in the electrode [6, 7]. Heusler alloys are named after Friedrich Heusler, a German engineer who initiated fundamental research in half-metalic ferromagnets compounds in 1903. This attempts the advantage to a new generation of devices that integrate standard microelectronics with spin-dependent effects, such as nonvolatile magnetic random access memories and magnetic sensors [8, 9]. Magnetic Heusler alloys have grown in popularity due to their multifunctional properties, which make them useful in a variety of domains ranging from spintronics to magnetic shape memory and magnetocaloric technologies [10–19]. The magnetic Heusler alloys strong magnetoelastic interactions are accountable for novel functional features such as magnetic shape memory and magnetocaloric effects [10,13,14]. Heusler alloys are a type of half-metallic magnetic material that is used in spintronic device applications [20]. Half metallic magnetic

materials with 100% spin polarization at the interface of the valence and conduction bands have received a lot of attention. Heusler alloys can be classified into two main groups, namely, Half-Heusler, full-Heusler alloys can be synthesized using the chemical formulations XYZ, X_2YZ respectively. Where X and Y represent transitional metal elements and Z represents a main group element [21]. Full-Heusler X_2YZ alloys generally have two types of structures, $CuHg_2Ti$ and $AlCu_2Mn$. Usually, the Heusler structure can be looked as four interpenetrating face centered cubic lattices and has four unique crystal sites namely A (0, 0, 0), B (0.25, 0.25, 0.25), C (0.5, 0.5, 0.5), and D (0.75, 0,75, 0.75) in Wyckoff coordinates. It is found that the site preference of the X and Y atoms is strongly influenced by the number of their valence electrons [22]. Many researches devoted to investigate the physical properties of Zr-based compounds such as: Zr_2CrZ (Z=Ga, In) with $CuHg_2Ti$-type structure [23]. In this work, we present an attempt of density functional theory (DFT) study for the Zr_2NiB alloys in order to enrich the Zr-based Heusle alloys. The paper is organized as follows: in chapter two, we explain the basic quantum mechanics and density functional theory, in chapter three, it includes the calculation methods and the structural, magnetic, electronic and optical properties are discussed; finally in chapter four, we summarize our calculated results and conclusions.

Chapter 2

Theoretical background

2.1 Schrödinger equation

The Schrödinger equation is a linear partial differential equation that governs the wave function of a quantum-mechanical system. It is a key result in quantum mechanics, and its discovery was a significant landmark in the develoment of subject, the name after Erwin Schrödinger [24].

$$\hat{H}\Psi(\vec{r}) = \hat{E}\Psi(\vec{r}) \tag{2.1}$$

Where $\hat{H}$ is the hamiltonian operator, and Ψ is the wave function. Using the Hamiltonian for a single particle

$$\hat{H} = \hat{T} + \hat{V} = -\frac{\hbar^2}{2m}\vec{\nabla}^2 + V(\vec{r}) \tag{2.2}$$

leads to the (non-relativistic) time-independent single-particle Schrödinger equation

$$\hat{E}\Psi(\vec{r}) = \left[-\frac{\hbar^2}{2m}\vec{\nabla}^2 + V(\vec{r}) \right]\Psi(\vec{r}). \tag{2.3}$$

For N particles in three dimensions, the Hamiltonian is

$$\hat{H} = \sum_{i=1}^{N} \frac{\hat{p}_i^2}{2m_i} + V(\vec{r}_1, \vec{r}_2, ...\vec{r}_N) = -\frac{\hbar^2}{2} \sum_{i=1}^{N} \frac{1}{m_i} + V(\vec{r}_1, \vec{r}_2, ...\vec{r}_N) \tag{2.4}$$

The corresponding Schrödinger equation reads

$$\hat{E}\Psi(\vec{r}_1, \vec{r}_2, ...\vec{r}_N) = \Big[-\frac{\hbar^2}{2} \sum_{i=1}^{N} \frac{1}{m_i} \nabla_i^2 + V(\vec{r}_1, \vec{r}_2, ...\vec{r}_N) \Big] \Psi(\vec{r}_1, \vec{r}_2, ...\vec{r}_N) \tag{2.5}$$

Special cases are the solutions of the time-independent Schrödinger equation, where the Hamiltonian itself has no time-dependency (which implies a time-independent potential V $((\vec{r}_1, \vec{r}_2, ...\vec{r}_N))$ and the solutions therefore describe standing waves which are called stationary states or orbitals). The time-independent Schrödinger equation is not only easier to treat, but the knowledge of its solutions also provides crucial insight to handle the corresponding time-dependent equation. The time-independent equation is obtained by the approach of separation of variables, i.e. the spatial part of the wave function is separated from the temporal part via [25]

$$\psi(\vec{r}_1, \vec{r}_2, ...\vec{r}_N, t) = \psi(\vec{r}_1, \vec{r}_2, ...\vec{r}_N, t)\tau(t) = \psi(\vec{r}_1, \vec{r}_2, ...\vec{r}_N) e^{\frac{iEt}{\hbar}} \tag{2.6}$$

Furthermore, the l.h.s. of the equation reduces to the energy eigenvalue of the Hamiltonian multiplied by the wave function, leading to the general eigenvalue equation

$$E\psi(\vec{r}_1, \vec{r}_2, ...\vec{r}_N) = \hat{H}\psi(\vec{r}_1, \vec{r}_2, ...\vec{r}_N)) \tag{2.7}$$

Again, using the many-body Hamiltonian, the Schrödinger equation becomes

$$E\psi(\vec{r}_1, \vec{r}_2, ...\vec{r}_N) = \Big[-\frac{\hbar^2}{2} \sum_{i=1}^{N} \frac{1}{m_i} \nabla_i^2 + V((\vec{r}_1, \vec{r}_2, ...\vec{r}_N) \Big] \psi(\vec{r}_1, \vec{r}_2, ..., \vec{r}_N) \tag{2.8}$$

2.2 The wave function

The wave function ψ has no direct physical meaning. The wave function $\psi(r,t)$ describes the position of a particle with respect to time. It can be considered as probability amplitude. $|\psi|^2$ is proportional to the probability of finding a particle at a particular time. It is the probability density [26, 27].

$$|\psi|^2 = |\psi^*\psi|^2 \tag{2.9}$$

For the sake of simplicity the discussion is restricted to the time-independent wave function. The Born probability interpretation of the wave function, which is a major principle of the Copenhagen interpretation of quantum mechanics, provides a physical interpretation for the square of the wave function as a probability density [28, 29]

$$P = |\psi(\vec{r}_1, \vec{r}_2, ...\vec{r}_N, t)|^2 d\vec{r}_1 d\vec{r}_2 .... d\vec{r}_N \tag{2.10}$$

Equation (2.10) describes the probability that particles 1,2,...,N are located simultaneously in the corresponding volume element $d\vec{r}_1\ d\vec{r}_2 ... d\vec{r}_N$ [30] . What happens if the positions of two particles are exchanged, must be considered as well. Following merely logical reasoning, the overall probability density cannot depend on such an exchange, i.e.

$$|\psi(\vec{r}_1, \vec{r}_2, ..., \vec{r}_i, \vec{r}_j, ..., \vec{r}_N)|^2 = |\psi(\vec{r}_1, \vec{r}_2, ..., \vec{r}_j, \vec{r}_i, ..., \vec{r}_N)|^2 \tag{2.11}$$

There are only two possibilities for the behavior of the wave function during a particle exchange. The first one is a symmetrical wave function, which does not change due to such an exchange. This corresponds to bosons (particles with integer or zero spin). The other possibility is an anti-symmetrical wave function, where an exchange of two particles causes a sign change, which corresponds to fermions (particles which half-integer spin) [26, 31]. Another consequence of the probability interpretation is the normalization of the wave function. If equation (2.10) describes the probability of finding a particle in a volume element, setting the full range of

coordinates as volume element must result in a probability of one, i.e. all particles must be found somewhere in space. This corresponds to the normalization condition for the wave function.

$$\int d\vec{r}_1 \int d\vec{r}_2 ... \int d\vec{r}_N |\psi(\vec{r}_1, \vec{r}_2, ..., \vec{r}_N)|^2 = 1 \tag{2.12}$$

Equation (2.12) also gives insight on the requirements a wave function must fulfill in order to be physical acceptable. Wave functions must be continuous over the full spatial range and square-integratable [32]. Calculating the expectation values of operators with a wave function also provides the expectation value of the relevant observable for that wave function [33]. For an observable $O(\vec{r}_1, \vec{r}_2, ..., \vec{r}_N)$, this can generally be written as

$$O = \langle O \rangle = \int d\vec{r}_1 \int d\vec{r}_2 ... \int d\vec{r}_N \psi^*(\vec{r}_1, \vec{r}_2, ..., \vec{r}_N) \hat{O} \psi(\vec{r}_1, \vec{r}_2, ..., \vec{r}_N) \tag{2.13}$$

2.3 Born-Oppenheimer (BO) approximation

The Hamiltonian of a many-body condensed-matter system consisting of nuclei and electrons can be written as:

$$\hat{H} = -\frac{\hbar^2}{2m_e} \sum_{i=1}^{N} \nabla i^2 - \frac{\hbar^2}{2M_k} \sum_{k=1}^{M} \nabla_k^2 - \sum_{i=1}^{N} \sum_{k=1}^{M} \frac{Z_k e^2}{r_{ik}} + \frac{1}{2} \sum i = 1^N \sum_{j>i}^{N} \frac{e^2}{r_{ij}} + \frac{1}{2} \sum_{k=1}^{M} \sum_{l>k}^{M} \frac{Z_k Z_l}{R_{kl}} \tag{2.14}$$

Using the Born-Oppenheimer approximation, the electrons in a molecule are described without taking into account the mobility of the atomic nuclei. It is based on the fact that the mass of a nucleus in a molecule is significantly greater than the mass of an electron (more than 1000 times) [34]. Consequently, the many-body problem is simplified to the smaller problem of a system of electrons traveling in an external potential, such as the potential formed by positively charged nuclei. The Schrödinger equation for this system is then

$$\hat{T}\psi + \hat{V}\psi = -i\hbar \frac{\partial \psi(\vec{x}, t)}{\partial t} \tag{2.15}$$

where ψ is the many-electron wavefunction. In electronic structure calculations, this is the most important object to consider because it holds all of the information about the system of electrons. A probability amplitude for discovering a system of electrons in a given configuration is provided by this formula,

$$\psi = \psi(\vec{r}_1, \vec{r}_2, ...\vec{r}_n) \tag{2.16}$$

where the $\vec{r}_n$ are the coordinates of the electrons. Again, spin is included in the coordinates $\vec{r}_n$, so that ($\vec{r} = (x, y, z, \sigma)$ where σ is the spin coordinate and can take the values of ($\uparrow$ spin-up) or ($\downarrow$ spin-down). $\hat{T}$ is now the many-electron kinetic energy operator, acting on as

$$\hat{T}\psi = -\frac{1}{2} \bigtriangledown^2 \vec{r}_n \psi \tag{2.17}$$

$\bigtriangledown^2 \vec{r}_n$ is the many-electron potential operator, which acts on ψ as

$$\hat{V}\psi = -\frac{1}{2} \left(\sum_n \bigtriangledown^2_{n \neq m} \mid \frac{1}{\vec{r}_n - m_n} \mid + v_{ext}(\vec{r}_n) \right) \psi \tag{2.18}$$

where V_{ext} is the external potential in which the electrons are moving. For the system of electrons and nuclei is given by,

$$V_{ext}((\vec{r}) = -\sum_{n,m} \mid \frac{Z_{l_m}}{(\vec{r}_n - R_{ln}} \mid \tag{2.19}$$

It leads to the easy method for the treatment of molecules. The Born-Oppenheimer is based on the fact that nuclei are several thousand times heavier than electrons. The proton, itself, is approximately 2000 times more massive than an electron. In a dynamical sense, the electrons can be regarded as particles that follow the nuclear motion adiabatically,meaning that they are dragged along with the nuclei without requiring a finite relaxation time. The many-electron Schrödinger equation must be solved in accordance with the limitations of normalization and exchange anti-symmetry. As a result of normalization, any potential electron configuration is

guaranteed to have the same probability to 1.

$$\psi(\vec{r}_1, \vec{r}_2, ..\vec{r}_n, \vec{r}_m, \vec{r}_N) = -\psi(\vec{r}_1, \vec{r}_2, ..\vec{r}_n, \vec{r}_m, \vec{r}_N) \tag{2.20}$$

Most of the time, we're solely concerned with the electronic system's ground state. This is the lowest-energy solution to the Schrödinger equation for Time-independent many-electron systems.

$$\hat{T}\psi + \hat{V}\psi = E\psi \tag{2.21}$$

where E is the ground state energy of the system of electrons.

2.4 The Hartree-Fock approach

In order to find a suitable strategy to approximate the analytically not accessible solutions of many-body problems, a very useful tool is variational calculus, similar to the least-action principle of classical mechanics. By the use of variational calculus, the ground state wave function ψ_0 , which corresponds to the lowest energy of the system E_0 , can be approached [35]. Hence, for now only the electronic Schrödinger equation is of interest, therefore in the following sections we set $\hat{H} \equiv \hat{H}_e l$, $E \equiv E_e l$, and so on. Observables in quantum mechanics are calculated as the expectation values of operators [25, 28]. The energy as observable corresponds to the Hamilton operator, therefore the energy corresponding to a general Hamiltonian can be calculated as

$$E = \langle \hat{H} \rangle = \int d\vec{r}_1 \int d\vec{r}_2 ... \int d\vec{r}_N \psi * (\vec{r}_1, \vec{r}_2, ..., \vec{r}_N) \hat{H} \psi(\vec{r}_1, \vec{r}_2, ..., \vec{r}_N) \tag{2.22}$$

The Hatree-Fock techique is based on the principle that the energy obtained by any (normalized) trial wave function other than the actual ground state wave function is always an upper bound, i.e. higher than the actual ground state energy. If the trial function happens to be the desired ground state wave function, the energies

are equal

$$E_{trial} \geq E_0 \tag{2.23}$$

with

$$E_{trial} = \int d\vec{r}_1 \int d\vec{r}_2 ... \int d\vec{r}_N \psi^*_{trial}(\vec{r}_1, \vec{r}_2, ..., \vec{r}_N) \hat{H} \psi_{trial}(\vec{r}_1, \vec{r}_2, ..., \vec{r}_N) \tag{2.24}$$

and

$$E_0 = \int d\vec{r}_1 \int d\vec{r}_2 ... \int d\vec{r}_N \psi^*_0(\vec{r}_1, \vec{r}_2, ..., \vec{r}_N) \hat{H} \psi_0(\vec{r}_1, \vec{r}_2, ..., \vec{r}_N) \tag{2.25}$$

For a detailed description of this notation, the reader is referred to the original publication [36]. In that notation, equation (2.23) to (2.25) are expressed as

$$\langle \psi_{trial} | \hat{H} | \psi_{trial} \rangle = E_{trial} \geq E_0 = \langle \psi_0 | \hat{H} | \psi_0 \rangle \tag{2.26}$$

Proof: [28] The eigenfunctions ψ_i of the Hamiltonian $\hat{H}$ (each corresponding to an energy eigenvalue E_i form a complete basis set, therefore any normalized tria wave function ψ_{trial}can be expressed as linear combination of those eigenfunctions.

$$\psi_{trial} = \sum_i \lambda_i \psi_i \tag{2.27}$$

The assumption is made that the eigenfunctions are orthogonal and normalized. Hence it is requested that the trial wave function is normalized, it follows that

$$\langle \psi_{trial} | \psi_{trial} \rangle = 1 = \langle \sum_i \lambda_i \psi_i | \sum_j \lambda_j \psi_j \rangle = \sum_i \sum_j \lambda^*_i \lambda_j \langle \psi_i | \psi_j \rangle = \sum_j |\lambda_j|^2 \tag{2.28}$$

On the other hand, following (2.23) and (2.25)

$$E_{trial} = \langle \psi_{trial} | \hat{H} | \psi_{trial} \rangle = \langle \sum_i \lambda_i \psi_i | \hat{H} | \sum_j \lambda_j \psi_j \rangle = \sum_j E_j |\lambda_j|^2 \tag{2.29}$$

Together with the fact that the ground state energy E_0 is per definition the lowest possible energy, and therefore has the smallest eigenvalue ($E_0 \leq E_i$), it is found that

$$E_{trial} = \sum_j E_j |\lambda_j|^2 \geq E_0 \sum_j |\lambda_j|^2 \tag{2.30}$$

what resembles equation (2.26). Equations(2.22) to (2.30) also include that a search for the minimal energy value while applied on all allowed N-electron wave-functions will always provide the ground-state wave function (or wave functions, in case of a degenerate ground state where more than one wave function provides the minimum energy). Expressed in terms of functional calculus,where $\psi \rightarrow N$ addresses all allowed N-electron wave functions,

$$E_0 = \min_{\psi \rightarrow N} E[\psi] = \min_{\psi \rightarrow N} \langle \psi | \hat{H} | \psi \rangle = \min_{\psi \rightarrow N} \langle \psi | \hat{T} + \hat{V} + \hat{U} | \psi \rangle \tag{2.31}$$

Due to the vast number of alternative wave functions on the one hand and processing power and time constraints on the other, this search is essentially unfeasible for N-electron systems. Restriction of the search to a smaller subset of potential wave functions, as in the Hartree-Fock approximation, is conceivable. A slater determinant is a formula in quantum mechanics that desceibes the wave function of a multi-fermionic system. It satisfies anti-symmetric criteria, and thus the Pauli's principle, by changing sign when two electrons are exchanged (or other fermions). Only a small fraction of all potential fermionic wave functions can be expressed as a single slater determinant, but because of their simplicity, they are an important and useful subset. In the Hartree- Fock approach, the search is restricted to approximations of the N-electron wave function by an antisymmetric product of N (normalized) one electron wave functons, the so called spin- orbitals $\chi_i(\vec{x}_i)$ [31]. A wave function of this type is called Slater-determinant, and reads.

$$\Psi_0 \approx \phi_{SD} = (N!)^{-\frac{1}{2}} \begin{vmatrix} \chi_1(\vec{x}_1) & \chi_2(\vec{x}_1) & \cdots & \chi_N(\vec{x}_1) \\ \chi_1(\vec{x}_2) & \chi_2(\vec{x}_2) & \cdots & \chi_N(\vec{x}_2) \\ \vdots & \vdots & \ddots & \vdots \\ \chi_1(\vec{x}_N) & \chi_2(\vec{x}_N) & \cdots & \chi_N(\vec{x}_N) \end{vmatrix} \tag{2.32}$$

It is important to notice that the spin-orbitals $\chi_i(\vec{x}_i)$ are not only depending on spatial coordinates but also on a spin coordinate which is introduced by a spin function, $\vec{x}_i = \vec{r}_i, s$. Returning to the variational principle and equation (2.31), the ground state energy approximated by a single slater determinant becomes.

$$E_0 = \min_{\phi_{SD} \to N} E[\phi_{SD}] = \min_{\phi_{SD} \to N} \langle \phi_{SD} | \hat{H} | \phi_{SD} \rangle = \min_{\phi_{SD} \to N} \langle \phi_{SD} | \hat{T} + \hat{V} + \hat{U} | \phi_{SD} \rangle \tag{2.33}$$

A general expression for the Hartree-Fock Energy is obtained by usage of the Slater determinant as a trial function.

$$E_{HF} = \langle \phi_{SD} | \hat{H} | \phi_{SD} \rangle = \langle \phi_{SD} | \hat{T} + \hat{V} + \hat{U} | \phi_{SD} \rangle \tag{2.34}$$

For the sake of brevity, a detailed derivation of the final expression for the Hartree-Fock energy is omitted. It is a straightforward calculation found for example in the Book by Schwabl [25]. The final expression for the Hartree-Fock energy contains three major parts: [31].

$$E_{HF} = \langle \phi_{SD} | \hat{H} | \phi_{SD} \rangle = \sum_{i}^{N} (i|\hat{h}|i) + \frac{1}{2} \sum_{i}^{N} \sum_{j}^{N} [(ii|jj) - (ij|ji)] \tag{2.35}$$

with

$$(i|\hat{h}_i|i) = \int \chi_i^*(\vec{x}_i)[-\frac{1}{2}\vec{\nabla}_i^2 - \sum_{k=1}^{M} \frac{Z_k}{r_{ik}}]\chi_i(\vec{x}_i) d\vec{x}_i, \tag{2.36}$$

$$(ii|jj) = \iint |\chi_i(\vec{x}_i)|^2 \frac{1}{r_{ij}} |\chi_j(\vec{x}_j)|^2 d\vec{x}_i d\vec{x}_j, \tag{2.37}$$

$$(ii|jj) = \iint \chi_i(\vec{x}_i)\chi_j^*(\vec{x}_j)\frac{1}{r_{ij}}\chi_j(\vec{x}_j)\chi_i^*(\vec{x}_i)d\vec{x}_i d\vec{x}_j \tag{2.38}$$

The first term corresponds to the kinetic energy and the nucleus-electron interactions, $\hat{h}$ denoting the single particle contribution of the Hamiltonian, whereas the latter two terms correspond to electron-electron interactions. They are called Coulomb and exchange integral, respectively. Examination of equations (2.35) to (2.38) furthermore reveals, that the Hartree-Fock energy can be expressed as a functional of the spin orbitals $E_{HF} = E[\{\chi_i\}]$. Thus,variation of the spin orbitals leads to the minimum energy. An important point is that the spin orbitals remain orthonormal during minimization.This restriction is accomplished by the introduction of Lagrangian multipliers λ_i in the resulting equations, which represent the Hartree-Fock equations.

$$\hat{f}\chi_i = \lambda_i\chi_i \qquad i = 1, 2, ..., N \tag{2.39}$$

with

$$\hat{f}_i = -\frac{1}{2}\vec{\nabla}_i^2 - \sum_{k=1}^{M}\frac{Z_k}{r_{ik}} + \sum_{i}^{N}[\hat{J}_j(\vec{x}_i) - \hat{K}_j(\vec{x}_i)] = \hat{h}_i + \hat{V}^{HF}(i) \tag{2.40}$$

Finally one arrives at the Fock operator for the i-th electron. In similarity to(2.28) to (2.31), the first twonterms represent the kinetic and potential energy due to nucleus-electron interaction, collected in the core Hamiltonian $\hat{h}_i$, whereas the latter terms are sums over the Coulomb operators $\hat{J}_j$ and the exchange operators $\hat{K}_j$ with the other j electrons, which form the Hartree-Fock potential $\hat{V}^{HF}$. There are major approximation of Hartree-Fock can be seen. The two electron repulsion operator from the original Hamiltonian is exchanged by a one-electron operator $\hat{V}^{HF}$ which describes the repulsion in average.

2.4.1 Limitations and failings of the Hartree-Fock approach

Atoms as well as molecules can have an even or odd number of electrons. If the number of electrons is even and all of them are located in double occupied spatial

orbitals ϕ_i, the compound is in a singlet state.Such systems are called *closed-shell systems*. Compounds with an odd number of electrons as well as compounds with single occupied orbitals, i.e. species with triplet or higher ground state, are called *open-shell systems* respectively. These two types of systems correspond to two different approaches of the Hartree-Fock method. In the *restricted* HF-method (RHF),all electrons are considered to be paired in orbitals whereas in the *unrestricted* HF (UHF)-method this limitation is lifted totally. It is also possible to describe open-shell systems with a RHF approach where only the single occupied orbitals are excluded which is then called a *restricted open-shell* HF (ROHF) which is an approach closer to reality but also more complex and therefore less popular than UHF [31].

There are also closed-shell systems which require the unrestricted approach in order to get proper results. For instance, the description of the dissociation of H_2 (i.e. the behavior at large internuclear distance), where one electron must be located at one hydrogen atom, can logically not be obtained by the use of a system which places both electrons in the same spatial orbital. Therefore the choice of method is always a very important point in HF calculations [37].Kohn states several $M = p^5$ with $3 \leq p \leq 10$ parameters for an output with adequate accuracy in the investigations of the H_2 system [38]. For a system with $N = 100$ electrons, the number of parameters rises to,

$$M = p^{3N} = 3^{300} to 10^{300} \approx 10^{150} to 10^{300} \tag{2.41}$$

According to the equation (2.41), energy reduction would have to be done in a space with at least 10^{150} dimension, which is well above current computer capabilities. As a result, HF methods are limited to situations involving a modest number of electron ($N \approx 10$), This barrier commonly referred to as the exponential wall because of the exponential component in (2.41) [38]. Since a many electron wave function cannot be described entirely by a single Slater determinant, the energy obtained by HF calculations is always larger than the exact ground state energy. The most accurate energy obtainable by HF-methods is called the *Hartree-Fock-limit*.

The difference between E_{HF} and E_{exact} is called *correlation energy* and can be

denoted as [39]

$$E_{corr}^{HF} = E_{min} - E_{HF} \tag{2.42}$$

$$E_{corr}^{HF} = 14.9eV < 0.001.E_{min}, \tag{2.43}$$

it can have a huge influence.

$$E_{diss} = 9.9eV < E_{corr}, \tag{2.44}$$

2.5 The electron density

A general statement concerning the computation of observables has been presented in section about the wave function ψ. This section is about a quantity that is computed in a similar manner. The electron density (for N electrons) as the as [27].

$$n(\vec{r}) = N \sum_{s_1} \int d\vec{x}_2 ... \int d\vec{x}_N \psi^*(\vec{x}_1, \vec{x}_2, ..., \vec{x}_N)\psi(\vec{x}_1, \vec{x}_2, ..., \vec{x}_N). \tag{2.45}$$

Which is the basic variable of density function theory. If the spin coordinates are neglected, the electron density can even be expressed as measurable observable only dependent on spatial coordinates.

$$n(\vec{r}) = N \int d\vec{r}_2 ... \int d\vec{r}_N \psi^*(\vec{r}_1, \vec{r}_2, ..., \vec{r}_N)\psi(\vec{r}_1, \vec{r}_2, ..., \vec{r}_N) \tag{2.46}$$

The total number of electrons can be obtained by integration the electron density over the spatial variables. which can e.g. be measured by X-ray diffraction.

$$N = \int d\vec{r} n(\vec{r}). \tag{2.47}$$

2.6 Thomas-Fermi Model

The predecessor to DFT was the Thomas-Fermi (TF) model proposed by Thomas amd Fermi [40] in 1927. In this method, they used the electron density $n(\mathbf{r})$ as

the basic variable instead of the wave function. The total energy of a system in an external potential $V_{ext}(\mathbf{r})$ is written as a function of the electron density $n(\mathbf{r})$ as:

$$E_{TF}[n(\mathbf{r})] = A_1 \int n(\mathbf{r})^{\frac{5}{3}} d\vec{r} + \int n(\mathbf{r}) V_{ext}(\mathbf{r}) d\mathbf{r} + \frac{1}{2} \iint \frac{n(\mathbf{r}) n(\mathbf{r}')}{|\mathbf{r} - \mathbf{r}'|} d\mathbf{r} d\mathbf{r}' \qquad (2.48)$$

where the first term is the kinetic energy of the non-interacting electron in a homogeneous electron gas (HEG) with $A_1 = \frac{3}{10}(3\pi^2)^{\frac{2}{3}}$ in the atomic units. The free electron energy state $\varepsilon_k = \frac{k^2}{2}$ up to the fermi wave vector $k_F = [3\pi^2 n(\vec{r})]^{\frac{1}{3}}$ as:

$$t_0[n(\mathbf{r})] = \frac{2}{(2\pi)^3} \int_0^{k_F} \frac{k^2}{2} 4\pi k^2 dk = A_1 n(\mathbf{r})^{\frac{5}{3}} \qquad (2.49)$$

In 1930, Dirac extended the Thomas-Fermi method by adding a local exchange term $A_2 \int n(\vec{r})^{\frac{3}{4}} d\vec{r}$ to Eq.(2.48) with $A_2 = -\frac{3}{4}(\frac{3}{\pi})^{\frac{1}{3}}$ which leads Eq.(2.48) to

By using the technique of Lagrange multipliers, the solution can be found in the stationary condition:

$$\delta\{E_{TED}[n(\mathbf{r})] - \mu(\int n(\mathbf{r}) - N)\} = 0 \qquad (2.50)$$

where μ is a constant known as a Lagrange multiplier, whose physical meaning is the chemical potential. E.(2.51) leads to the Thomas-Fermi-Dirac equation,

$$\frac{5}{3} A_1 n(\vec{r})^{\frac{2}{3}} + V_{ext}(\mathbf{r}) + \int \frac{n(\mathbf{r}')}{|(\mathbf{r}) - (\mathbf{r})'|} d(\mathbf{r})' + \frac{4}{3} A_2 n(\mathbf{r}))^{\frac{1}{3}} - \mu = 0 \qquad (2.51)$$

This can be solved directly to obtain the ground state density. Although it is not good enough to describe electrons in matter.

2.7 The Hohenberg-Kohn (HK) theorems

DFT was proven to be an exact theory of many-body systems by Hohenberg and Kohn [41] in 1964. It applies not only to condensed-matter systems of electrons with fixed nuclei, but also more to any system of interacting particles in an external potential $V_{ext}(\mathbf{r})$. The theory is based upon two theorems.

2.7.1 The HK theorem I

The ground state particle density $n(\mathbf{r})$ of a system of interacting particles in an external potential $V_{ext}(\mathbf{r})$ uniquely determines the external potential $V_{ext}(\mathbf{r})$, except for a constant. Thus the ground state particle density determines the full Hamiltonian, except for a constant shift of the energy. In principle, all the states including ground and excited states of the many-body wave functions can be calculated. This means that the ground state particle density uniquely determines all properties of the system completely.

Here only consider the case that the ground state of the system is nondegenerate. It can be proven that the theorem is also valid for systems with degenerate ground state. Suppose there are two different external potentials $V_{ext}(\mathbf{r})$ and $V_{ext}(\mathbf{r})'_{ext}(\mathbf{r})$ whice differ by more than a constant and lead to the same ground state density $n_0(\mathbf{r})$. The two external potentials would give two different Hamiltonians, Ψ and Ψ', with $\hat{H}\Psi = E_0\Psi$ and $\hat{H}'\Psi' = E'_0\Psi'$. Since Ψ' is not the ground state of $\hat{H}$, it follows that

$$\begin{aligned} E_0 &< \langle\Psi'|\hat{H}|\Psi'\rangle \\ &< \langle\Psi'|\hat{H}'|\Psi'\rangle + \langle\Psi'|\hat{H} - \hat{H}'|\Psi'\rangle \\ &< E'_0 + \int n_0(r)[V_{ext}(r) - V'_{ext}(r)]dr \end{aligned} \tag{2.52}$$

Similarly

$$\begin{aligned} {E_0}' &< \langle\Psi|\hat{H}'|\Psi\rangle \\ &< \langle\Psi|\hat{H}|\Psi\rangle + \langle\Psi|\hat{H}' - \hat{H}|\Psi\rangle \\ &< E_0 + \int n_0(r)[V'_{ext}(r) - V_{ext}(r)]dr \end{aligned} \tag{2.53}$$

Adding Eq. (2.44) and (2.45) lead to the contradiction

$$E_0 + E'_0 < E_0 + E'_0 \tag{2.54}$$

Hence, no two different external potentials $V_{ext}(\mathbf{r})$ can give rise to the same ground state density $n_0(\mathbf{r})$,i.e., the ground state density determines the external potential $V_{ext}(\mathbf{r})$, except for a constant.That is to say, there is a one-to-one mapping between the ground state density $n_0(\mathbf{r})$ and the external potential $V_{ext}(\mathbf{r})$, although the exact formula is known.

2.7.2 The HK theorem II

There exists a universal functional $F[n(\mathbf{r})]$ of the density, independent of external potential $V_{ext}(\mathbf{r})$, such that the global minimum value of the energy functional $E[n(\mathbf{r})] \equiv \int n(\mathbf{r})V_{ext}(V)d(\mathbf{r}) + F[n(\mathbf{r})]$ is the exact ground state energy of the system and the exact ground state density $n_0(\mathbf{r})$ minimizes this functional. Thus the exact ground state energy and density are fully determined by the functional $E[n(\mathbf{r})]$.

The universal functional $F[n(\mathbf{r})]$ can be written as

$$F[n(\mathbf{r})] \equiv T[n(\mathbf{r})] + E_{int}[n(\mathbf{r})] \tag{2.55}$$

where $T[n(\mathbf{r})]$ is the kinetic energy and $Eint[n(\mathbf{r})]$ is the interaction energy of the particles. According to variational principle, for any wave function Ψ', the energy functional $E[\Psi']$:

$$E[\Psi'] = \langle \Psi' | \hat{T} + \hat{V}_{int} + \hat{V}_{ext} | \Psi' \rangle \tag{2.56}$$

has its global minimum value only when Ψ' is the ground state wave function Ψ_0, with the constraint that the total number of the particles is conserved. According to HK theorem I, $\Psi\prime$ must correspond to a ground state with particle functional of $n'(\vec{r})$ and external potential $V'_{ext}(r)$, then $E[\Psi']$ is a functional of $n\prime(\mathbf{r})$. According to variational principle:

$$\begin{aligned} E[\Psi'] &\equiv \langle \Psi' | \hat{T} + \hat{V}_{int} + \hat{V}_{ext} | \Psi' \rangle \\ &= E[n\prime(\mathbf{r})] \\ &= \int n'(\mathbf{r}) V'_{ext}(\mathbf{r}) d\mathbf{r} + F[n'(\mathbf{r})] \end{aligned}$$

$$> E[\Psi_0] \tag{2.57}$$

$$= \int n_0(\mathbf{r}) d(\mathbf{r}) + F[n_0(\mathbf{r})] = E[n_0(\mathbf{r})]$$

Thus the energy functional $E[n(\mathbf{r})] \equiv \int n(\mathbf{r}) V_{ext}(\mathbf{r}) d(\mathbf{r}) + F[n(\mathbf{r})]$ evaluated for the correct ground state density $n_0(\mathbf{r})$ is indeed lower than the value of this functional for any other density $n(\mathbf{r})$. Therefore by minimizing the total energy functional of the system with respect to variations in the density $n(\mathbf{r})$, one would find the exact ground state density and energy.

2.8 The Kohn-Sham (KS) equations

Kohn and Sham introduced an orbital approach for evaluating $F_{ni}[n]$ in 1965, which was an important step toward quantitative modeling of electronic structure. In other words, in order to evaluate the kinetic energy of N non interacting particles given only their density distribution $n(\mathbf{r})$, they simply found the corresponding potential, called $v_{eff}(\mathbf{r})$, and used the Schrödinger equation.

$$\left(-\frac{\hbar^2}{2m}\vec{\nabla}^2 + v_{eff}(\mathbf{r}) \right) \psi_i(\mathbf{r}) = \epsilon_i \psi_i(\mathbf{r}) \tag{2.58}$$

Such that $n(\mathbf{r}) = \sum_{i=1}^{N} |\psi(\mathbf{r})|^2$ the states ψ_i here are ordered so that the energies ϵ_i are non decreasing, and the spin index is included in i. If the ϵ_N is degenerate with ϵ_{N+1} (and also at finite temperatures), fractional occupations f_i are to be used $n(\mathbf{r}) = \sum_{i=1}^{\infty} f_i |\psi(\mathbf{r})|^2$, but if only spin degeneracy is involved, the result for the density is not affected. The kinetic energy is then given by,$F_{ni} = \sum_{i=1}^{N} |\langle \psi_i | \hat{t} | \psi_i \rangle = \sum_{i=1}^{N} \epsilon_i - \int d(\mathbf{r}) n(\mathbf{r}) v_{eff}(\mathbf{r})$ where $\hat{t}_i$ is the kinetic energy operator for the ith electron ($\hat{T} = \sum_i \hat{t}_i$).

In practice, it is the external potential of a given system which is known, not the density distribution or the effective potential. One may find the effective potential by taking a functional derrivative of the three term expression for $F_{HK}[n]$, and

rearranging the terms:

$$v_{eff}(\mathbf{r}) = v(\mathbf{r}) - e\varphi(\mathbf{r}) + XC(\mathbf{r}) \tag{2.59}$$

where we have used equqtion (2.59)for both the interacting and non interacting system. The electrostatic potential is here

$$\varphi(\mathbf{r}) = -e \int d\mathbf{r}' \frac{n(\mathbf{r}')}{|\mathbf{r} - (\mathbf{r}')|} \tag{2.60}$$

And the exchange - correlation potential is defined as

$$v_{XC}(\mathbf{r}) = \frac{\delta E_{XC}}{\delta n(\mathbf{r})} \tag{2.61}$$

Given a particular approximation for $E_{XC}(n)$, one obtains $v_{XC}(\mathbf{r})$ and can thus find $v_{eff}(\mathbf{r})$ from $n(\mathbf{r})$ for a given $v(\mathbf{r})$. The set of equations described above is called the KohnSham equations of DFT [42]

2.8.1 Solving Kohn-Sham equations

Once we have approximated the exchange-correlation energy, we are in a position to solve the Kohn-Sham equations. The Kohn-Sham equations have an iterative solution; they have to be solved self-consistently. To solve the Kohn-Sham equations for a many body system, we need to define the Hartree potential and the exchange -correlation potential, and to define the Hartree potential and the exchange-correlation potential, we need to know the electron density $n(\mathbf{r})$.

However, to find the electron density, we must know the single electron wave functions. We do not know these wave functions until we solve the Kohn-Sham equations. The well-known approach to solve the Kohn-Sham equations is to start with an initial trial electron density as illustrated in figure 2.1. Then solve these equations using trial electron density. After solving the Kohn-Sham equations, we will have a set of single electron wave functions. Using these wave functions, we can calculate the new electron density. The new electron density in an input for the next cycle.

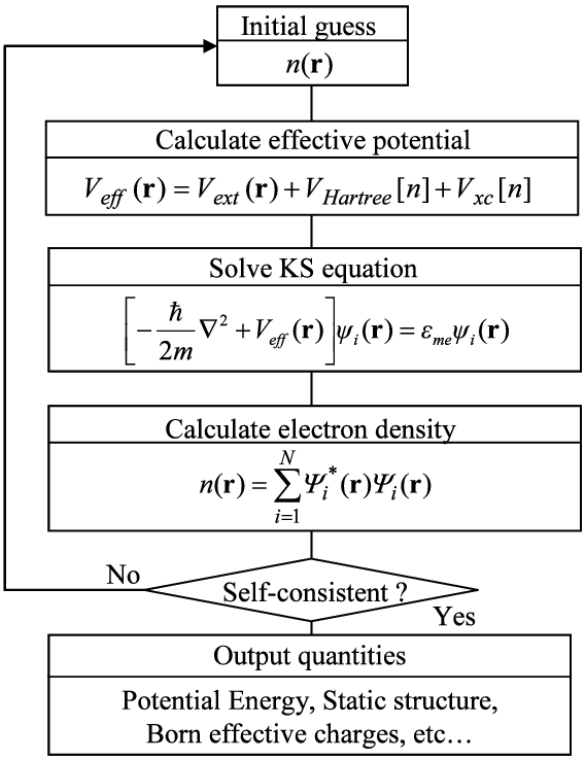

Figure 2.1: Flowchart of self-consistency loop for solving Kohn-Sham equations.

Finally, compare the difference between the calculated electron densities for consecutive iterations. If the difference in electron density between consecutive iteration is lower than an appropriately chosen convergence criterion, then the solution of the Kohn-Sham equations is said to be self-consistent. Now the calculated electron density is considered as the ground state electron density, and it can be used to calculate the total energy of the system [43]

2.9 The Exchange-Correlation (XC) functional

The exchange-correlation potential of the Kohn–Sham density-functional scheme is the difference between the Fermi potential an effective potential appearing in the one-electron Schrödinger equation for the square root of the electron density and the Pauli potential, i.e., vXC(r) = vF(r) − vP(r). The major problem in solving the Kohn-Sham equations is that the true form of the exchange-correlation functional is not known. Two main approximation methods have been implemented to approximate the exchange-correlation functional. The local density approximation (LDA) is first approach to approximate the exchange-correlation functional in DFT

calculations. The second well known class of approximations to the Kohn-Sham exchange-correlation functional is the generalized gradient approximation (GGA). In the GGA approximation the exchange and correlations energies include the local electron density and the local gradient in the electron density.

Chapter 3

Electronic, magnetic and optical properties

3.1 Computational Details

The electronic structure of our full-Heusler compound was calculated using the scalar relativistic FP-LAPW method within density functional theory as implemented in the WIEN2k code. Choosing a gradiant approximation for determining the exchange and correlation potential energy in the Kohn-Sham equation plays a significant role in the final result's accuracy. We use the Perdew-Burke-Ernzerhof (PBE) formulation of the generalized gradient approximation (GGA)to optimize the parameters namely $R_{MT}K_{max}$, K-points and lattice constant. The bassic functions are expended into spherical harmonic function inside the muffin-tin sphere and Furier series in the interstitial region. The convergence of the basis set was overseen by a cutoff parameter, $R_{MT}K_{max}=8$, where R_{MT} is the smallest radius of a muffin-tin sphere and K_{max} is the largest reciprocal lattice vector used in the plane wave expeansion within the interstitial region. The convergence of the total energy to a minimum value of 10^{-4} Ry determines the convergence of self-consistency calculations, while the charge convergence criteria was set 10^{-3} e. The number of K-points in the

Brillouin zone is approximately 10000.

3.2 Structural properties

Full Heusler compounds crystalize in two prototype structure. The regular Heusler crystallizes in a cubic structure $AlCu_2Mn$ prototype with the space group (225, $Fm\bar{3}m$) and the inverse Heusler, while in $CuHg_2Ti$ with space group (216, $F4\bar{3}m$). In the present work, we will study the full Heusler Zr_2NiB allow with $AlCu_2Mn$-type

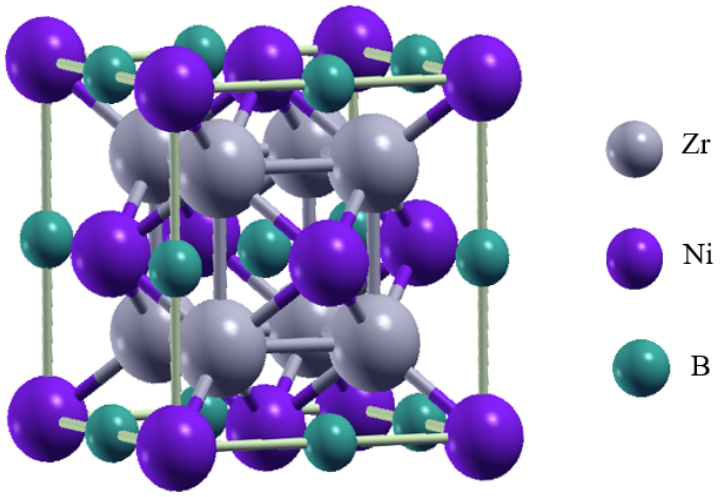

Figure 3.1: Crystal structure of the $AlCu_2Mn$-type for Zr_2NiB full-Heusler alloy.

structure, where Zr atoms occupy A (0, 0, 0) and C (0.5, 0.5, 0.5) Wyckoff positions while Ni and B atoms are respectively located at B (0.25, 0.25, 0.25) and D (0.75, 0.75, 0.75) positions. The full-Heusler compound consist of four interpenetrating face-centred-cubic lattices. Figure 3.1 gives a representation of this configuration. In order to obtain ground state of Zr_2NiB alloy, we firstly study the structural property using the plane-wave ultrasoft pseudo-potential DFT method. In fact, our basic procedure in this work is to calculate the total energy as a funtion of a unit-cell volume around a equilibrium state volume in the ferromagnetic (FM) phases. According to the modified Birch-Murnaghan equation of state volume optimization has been performed to obtain the ground state properties such as lattice parameter. The volume versus total energy plots of Zr_2NiB alloy are shown in Figure 3.2. The most stable structure of Zr_2NiB is confirmed by optimizing total energy as a function

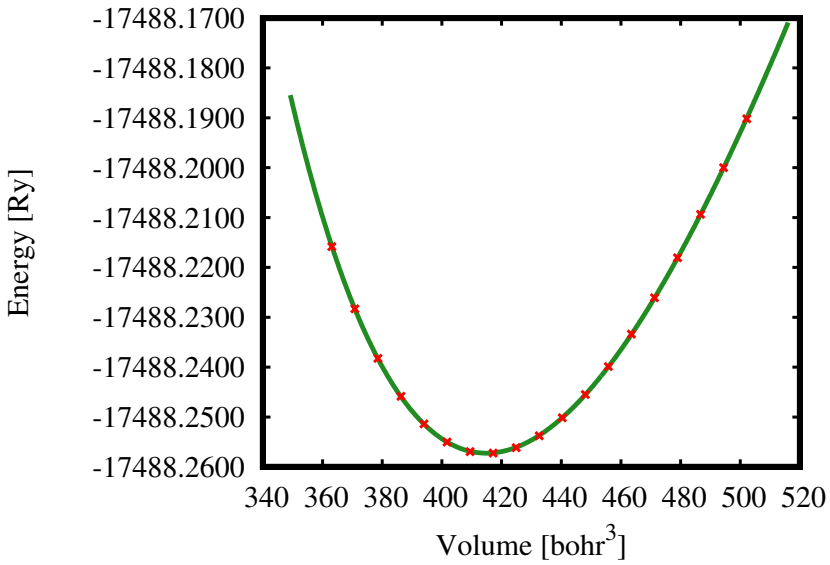

Figure 3.2: Calculated total energy of Zr_2NiB compound as a function of unit cell volume.

of volume for states with the lattice parameter 6.2656 Å. Figure 3.2, depicts the change of total energy with respect to cell volume in ferromagnetic states. Lattice constant is obtained from E-V, energy versus volume diagram where V is equilibrium volume. Table 3.1 the calculated Lattice Constant and Total energy.

Table 3.1: Minimun equilibrium energy, equilibrium lattice constant of Zr_2NiB for magnetic calculation.

Compounds	Structure type	Calculation	Lattice constant Å	Total energy (Ry)
Zr_2NiB	$AlCu_2Mn$	Magnetic	6.2656	-17488.25549092

3.3 Electronic properties

To comprehend the electronic properties of Zr_2NiB, we must compute the spin-polarized band structures and total density of states (TDOS) using the generalized gradient approximation (GGA) available as Perdew-Burke-Ernzerhof(PBE) funtional.

3.3.1 Band structures

The investigation of the electronic band structure is necessary to understand the physical properties of crystaline solids which almost completely describe optical as well as transport properties. Spin-polarized band structure of Zr_2NiB alloys at the

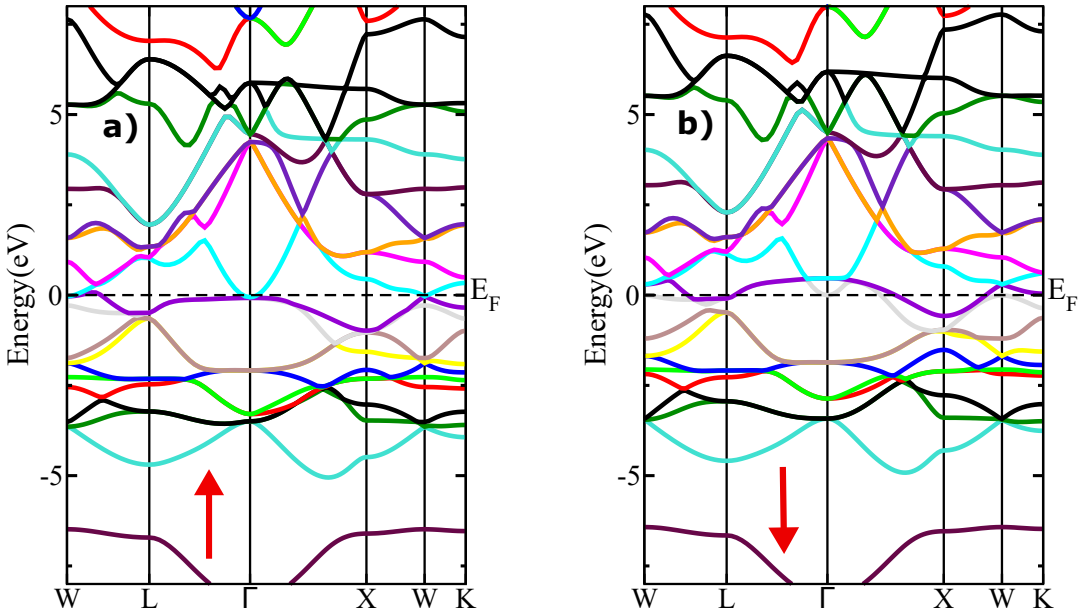

Figure 3.3: Band structures of full-Heusler Zr_2NiB a) spin up and b) spin down.

6.2656 Å lattice constant for both the spin-up and spin-down channels at equilibrium state along the high symmetry direction in the first Brillouin zone are illustrated in Figure 3.3(a) illustrated the spin-up (mejority) state and the Figure 3.3(b) sipn-down (minority) state respectively. Fermi level is set to zero. For the Zr_2NiB alloys, it's evidant that the valence bands overlap with conduction bands in both spin-up and spin-down band structure and the Fermi level passes through the overlapping region E_F. So the band gap is zero here. The minimum energy required to jump electron from majority spin channel to minority spin Fermi level, spin-flip gap Δ_{s-f} is 0 eV for Zr_2NiB. The zero flip gap for Δ_{s-f} which indicates these alloys are true metalic.

3.3.2 Density of states

The density of states (DOS) is essentially the number of different states that electrons are permitted to occupy at a given energy level, i.e. the number of electron states per unit volume per unit energy. For the study of electronic properties of

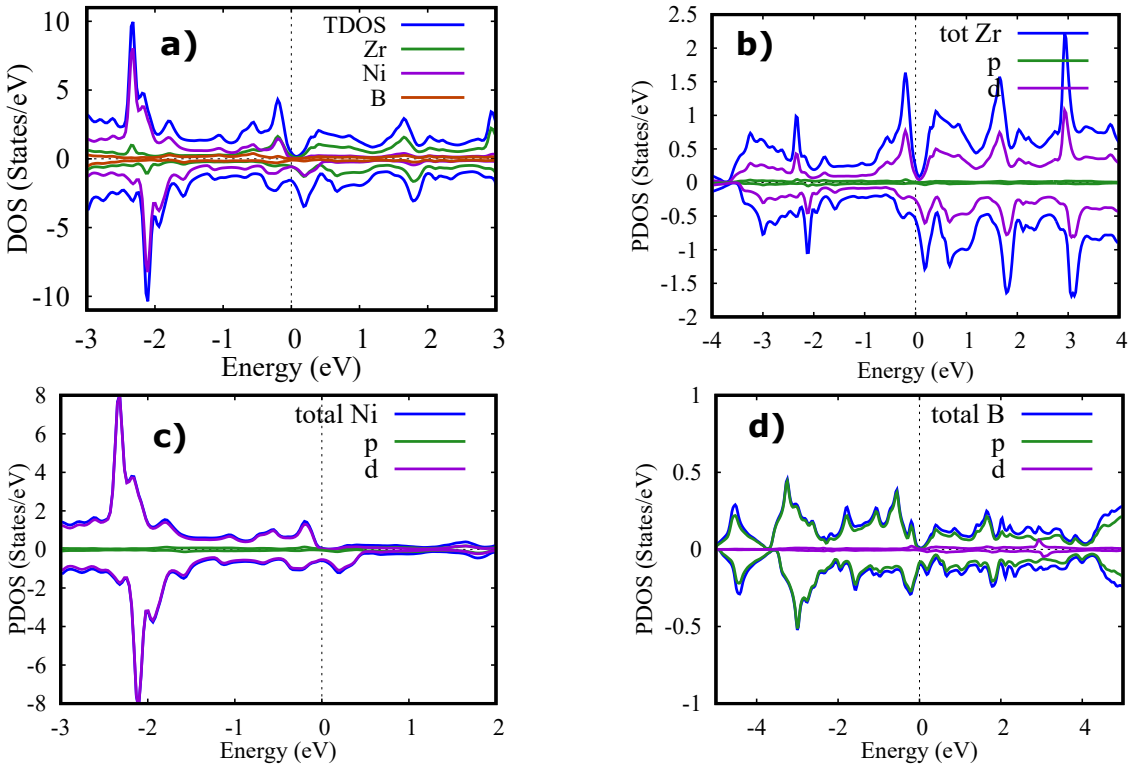

Figure 3.4: a) Total density of states (TDOS) and partial density of states (PDOS) of Zr_2NiB b) Zr c) Ni and d) B atoms

materials, it is necessary to calculated the total density of state (TDOS) and partial density states (PDOS) with GGA. The corresponding total and partial density of states for Zr_2NiB are illustrated in Figure 3.4(a-d). Now, the PDOS of Zr contains orbital p, d, electrons for the spin up and spin down for Zr_2NiB alloys is plotted in Figure 3.4(b). Similarly the PDOS of Ni and B are also plotted in Figure 3.4(c) and Figure 3.4(d). The upper portion depicts the majority spin density, while the lower portion depicts the minority spin density. For Zr_2NiB alloys, in Figure. 3.4(a) the conduction band overleps the Fermi level and enters into the valance band region, this indicates that the system is matelic.

3.4 Magnetic properties

The spin-polarized calculations show that the Zr_2NiB has ferromagnetic ordering. We have also calculated the partial magnetic moments of Zr, Ni, and B atoms, as well as the magnetic moment contribution of the interstitial region. We list the result

Table 3.2: Total spin magnetic moment of Zr_2NiB in PBA-GGA approach.

Compound	Structure type	Individual magnetic moment(μ_B)	
		Site	GGA
Zr_2NiB	$AlCu_2Mn$	Interstitial	0.21443
		M_{Zr}	0.19065
		M_{Ni}	0.38871
		M_B	0.01244
		M_{tot}	0.99688

in Table 3.2, The main contribution of total magnetic moment is due to Zr atoms. The partial moments of Zr and Ni are antiparallel that indicates the ferromagnetic of Zr_2NiB alloys. the calculated total magnetic moment for full Heusler alloys with $L2_1$ structure is an integer number 2.000 μ_B per formula unit which follows the Slater-Pauling (SP) rule: M_{tot}=(Z_{tot}-24) μ_B, where Z_{tot} represents the total number of valence electrons. This antiparallel alignment is beneficial to the Zr atoms leading to a total magnetic moment of $0.99\mu_B$. Ferromagnetic materials are commonly used for nonvolatile information storage in tapes, hard drives, etc.

3.5 Optical properties

Optical properties of a material define how it interacts with light. The response to electromagnetic radiation is important for optoelectronic device applications, so we have calculated the optical parameters of Zr_2NiB. We have calculated all the parameters using The GGA-PBE functional. In order to investigate the optical properties of Zr_2NiB full-Heusler alloys, we calculated its dielectric function, absorption coefficient, reflection, refraction and optical conductivity.

3.5.1 Dielectric function

The mathematical formula for dielectric function given by Ehrenreich and Cohen's is.

$$\epsilon(\omega) = \epsilon_1(\omega) + i\epsilon_2(\omega) \tag{3.1}$$

where, ϵ_1 and ϵ_2 are the real and imaginary part of the dielectric function. Real dielectric constant respectively, $(\epsilon_1(\omega))$ represents the degree of polarization of a material when it placed into an electric field and imaginary dielectric function $(\epsilon_2(\omega))$ represents the energy dissipation aptitude of a dielectric material. The optical response of the material to an electromagnetic field is described by the dielectric function. The real and imaginary dielectric function for Zr_2NiB obtained from PBE-GGA potential in Figure 3.5(a,b) where energy plotted in the X-direction, real and imaginary dielectric function ploted in Y-directin. The positive half is concerned with

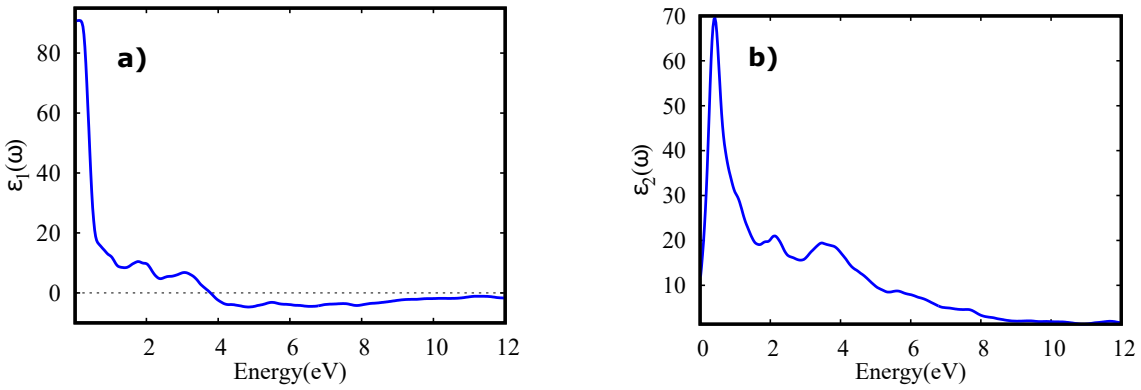

Figure 3.5: a) Real dielectric function b) Imaginary dielectric function

EM wave propagation, while the negative half is concerned with EM wave absorption. As a result, the larger the static value of $\epsilon_1(0)$, the smaller the magnitude of the band gap formed. The positive part of $\epsilon_1(\omega)$ indicates that Zr_2NiB conducts at low energy levels, while the negative part of $\epsilon_1(\omega)$ indicates that it is insulating at high energy levels.$\epsilon_1(\omega)$ begins to exhabit negative values at 3.85 eV and reaches its maximum negative values at 5.00 eV. From Figure 5.5(b) Zr_2NiB represent its peak value around 0.8 eV. Peaks represent charge carriers shifting from filled to empty bands. As energy increases, $\epsilon_2(\omega)$ begins to decrease and approaches zero at around 12 eV.

3.5.2 Absorption coefficient

The absorption coefficient is used to calculate how far into a material light of a specific wavelength can penetrate before being absorbed. Light is only poorly absorbed when a material has a low absorption coefficient.. Figures 3.6(c) represents the absorption coefficient of Zr_2NiB alloys. Peaks become more prominent around

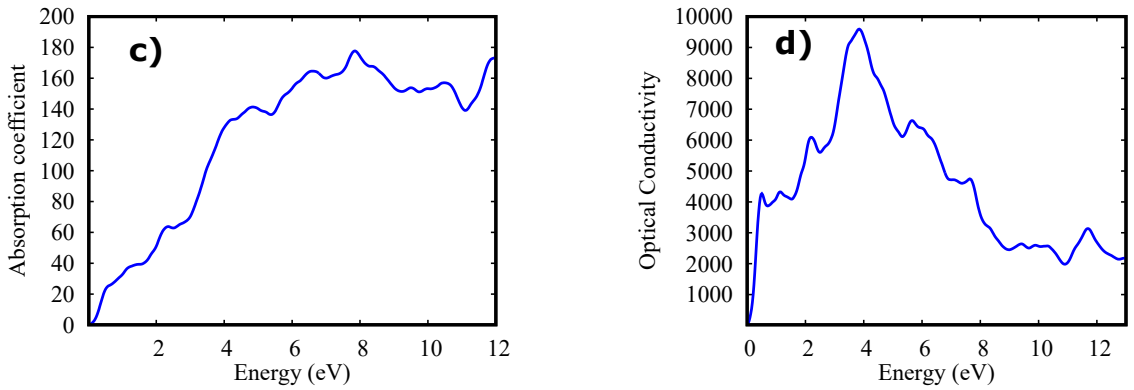

Figure 3.6: c) Absorption coefficient d) Optical conductivity

3 eV and continue to increase up to 11.1 eV, indicating that the highest value of Absorption Coefficient exists in the UV region.

3.5.3 Optical conductivity

Optical conductivity is a material property that describes the interaction between the induced current density in the material and the magnitude of the inducing electric field for arbitrarily selected frequencies. The optical conductivity along with its energy is illustrated in Figure 3.6(d). From the optical conductivity curve, it is obvious that conductivity increases as energy increases. The maximum conductivity peaks are obtained at 4 eV. Following an oscillatory trend, optical conductivity begins to decrease and eventually reaches zero for higher energy values. the optical curve reveals that the absorbed light spent the conductivity in the UV region.

3.5.4 Refractive index

The refractive index is another important physical quantity that describes the optical properties of any given material. The refractive index of a meterial, gives how much

a path of light is bent when it enters that material. It is also known that the

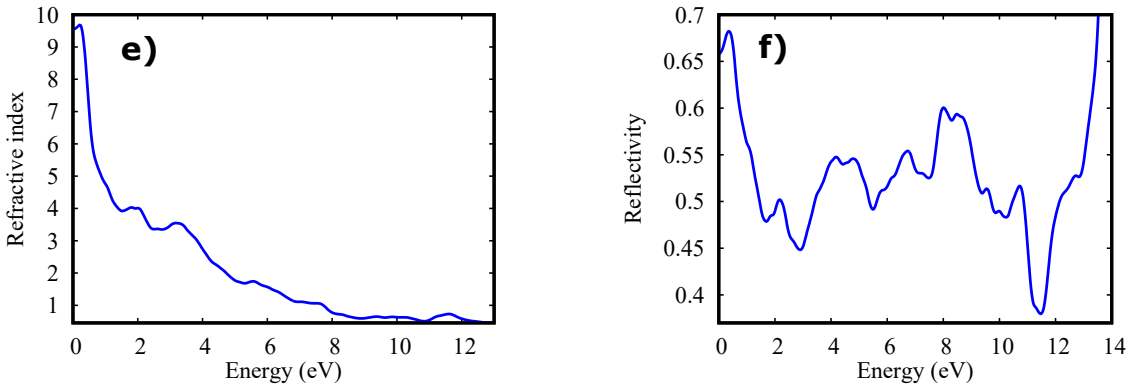

Figure 3.7: e) Refractive index f) Reflectivity

refractive indices are inversely related to the bandgap, if refractive index increases corresponding bandgap decreases. refractive index vs energy curve represent in Figure 3.7(e). It can be seen that in the low energy limit, the refractive index has a high value.. This indicated that increased the metallic behavior of Zr_2NiB alloy, efractive index deceases suddenly from the infrared region.

3.5.5 Optical reflectivity

The reflactance of a material is measured when light is incident on the surface of the material. The optical reflectivity plots show that the static values of reflectivity range from 0.66 to 0.68, with the reflectivity spectrum being minimum in the IR and visible regions and peaking in the vacuum UV region at higher energies. Reflectivity vs energy curve represent in Figure 3.7(f). Moreover, the reflectivity plots show the same behavior in the Near UV, Mid UV, and Deep UV regions. The greatest reflectivity is observed. The optical reflactivity is very high it represents the strong metallic characteristic of the Zr_2NiB compound.

Chapter 4

Conclusions

In this work, we have studied the structural properties phase of Zr_2NiB Heusler alloys using FP-LAPW method performed in WIEN2k code within GGA-PBE exchange correlation to survey the the structural, electronic, magnetic, and optical properties. According to the total energy versus unit cell volume diagram, the equilibrium lattice constant is found to be 6.2656Å. To investigate the investigate the electronic properties the diagrams of spin-polarized band structure of Zr_2NiB compounds and DOS, PDOS were plotted. Also found that these compounds for the spin-up and spin-down have no band gap that conforms their metalic properties. The Density of states also revealed the metalic nature of these compound. The obtained total magnetic moment for Full Heusler compounds was 0.99 μ_B. It is clear that that the value of the total magnetic moment is contributed by Zr atoms. In this work, also calculated optical properties using FP-LAPW method, the real and imaginary parts of dielectric function, reflectivity, absorption coefficient and optical conductivity. Curve of the real part of dielectric function versus energy show that there is metalic property in very low energies.

List of Abbreviations

BZ	:	Brillouin Zone
DFT	:	Density Functional Theory
DOS	:	Density of States
FP-LAPW	:	Full-Potential Linearized Augmented Plane Wave
GGA	:	Generalized Gradient Approximation
HF	:	Hartree-Fock
HK	:	Hohenberg-Kohn
HM	:	Half-Metallic
KS	:	Kohn-Sham
SP	:	Spin Polarization
XC	:	Exchange correlation

Bibliography

[1] PH Galanakis. Dederichs, and n. papanikolaou. *Phys. Rev. B*, 66(17):174429, 2002.

[2] Iosif Galanakis, Marjana Ležaić, Gustav Bihlmayer, and Stefan Blügel. Interface properties of ni mn sb/ in p and ni mn sb/ ga as contacts. *Physical Review B*, 71(21):214431, 2005.

[3] GY Gao, Lei Hu, KL Yao, Bo Luo, and Na Liu. Large half-metallic gaps in the quaternary heusler alloys cofecrz (z= al, si, ga, ge): A first-principles study. *Journal of alloys and compounds*, 551:539–543, 2013.

[4] GY Gao, Bin Xu, Zhi-Yuan Chen, and KL Yao. Surface d0 half-metallicity of rocksalt mgn from first-principles. *Journal of alloys and compounds*, 546:119–123, 2013.

[5] RA De Groot, FM Mueller, PG Van Engen, and KHJ Buschow. New class of materials: half-metallic ferromagnets. *Physical Review Letters*, 50(25):2024, 1983.

[6] Hideo Ohno. Making nonmagnetic semiconductors ferromagnetic. *science*, 281(5379):951–956, 1998.

[7] Sabine Wurmehl, Gerhard H Fecher, Hem Chandra Kandpal, Vadim Ksenofontov, Claudia Felser, and Hong-Ji Lin. Investigation of co 2 fe si: The heusler compound with highest curie temperature and magnetic moment. *Applied physics letters*, 88(3):032503, 2006.

[8] Gary A Prinz. Magnetoelectronics. *science*, 282(5394):1660–1663, 1998.

[9] JMD Coey, M Venkatesan, and MA Bari. ed c bertheir et al, 2002.

[10] Antoni Planes, Lluís Mañosa, and Avadh Saxena. Magnetism and structure in functional materials. 1, 2005.

[11] I Galanakis, Ph Mavropoulos, and Ph H Dederichs. Electronic structure and slater–pauling behaviour in half-metallic heusler alloys calculated from first principles. *Journal of Physics D: Applied Physics*, 39(5):765, 2006.

[12] Peter Entel, VD Buchelnikov, VV Khovailo, AT Zayak, WA Adeagbo, ME Gruner, HC Herper, and EF Wassermann. Modelling the phase diagram of magnetic shape memory heusler alloys. *Journal of Physics D: Applied Physics*, 39(5):865, 2006.

[13] Antoni Planes, Lluís Mañosa, and Mehmet Acet. Magnetocaloric effect and its relation to shape-memory properties in ferromagnetic heusler alloys. *Journal of Physics: Condensed Matter*, 21(23):233201, 2009.

[14] Markus E Gruner and Peter Entel. Impact of local lattice distortions on the structural stability of fe-pd magnetic shape-memory alloys. *Physical Review B*, 83(21):214415, 2011.

[15] Peter Entel, Antje Dannenberg, Mario Siewert, Heike C Herper, Markus E Gruner, Vasiliy D Buchelnikov, and Volodymyr A Chernenko. Composition-dependent basics of smart heusler materials from first-principles calculations. 684:1–29, 2011.

[16] Tanja Graf, Claudia Felser, and Stuart SP Parkin. Simple rules for the understanding of heusler compounds. *Progress in solid state chemistry*, 39(1):1–50, 2011.

[17] Tomoyuki Kakeshita, Takashi Fukuda, Avadh Saxena, and Antoni Planes. *Disorder and strain-induced complexity in functional materials*, volume 148. Springer Science & Business Media, 2011.

[18] Peter Entel, Mario Siewert, Markus E Gruner, Heike C Herper, Denis Comtesse, Raymundo Arróyave, Navedeep Singh, Anjana Talapatra, Vladimir V Sokolovskiy, Vasiliy D Buchelnikov, et al. Complex magnetic ordering as a driving mechanism of multifunctional properties of heusler alloys from first principles. *The European Physical Journal B*, 86(2):1–11, 2013.

[19] Peter Entel, Antje Dannenberg, Mario Siewert, Heike C Herper, Markus E Gruner, Denis Comtesse, Hans-Joachim Elmers, and Michael Kallmayer. Basic

properties of magnetic shape-memory materials from first-principles calculations. *Metallurgical and Materials Transactions A*, 43(8):2891–2900, 2012.

[20] KA Kilian and RH Victora. Electronic structure of ni 2 mnin for use in spin injection. *Journal of Applied Physics*, 87(9):7064–7066, 2000.

[21] Friedrich Heusler. Über magnetische manganlegierungen. *Verh. Dtsch. Phys. Ges*, 5(12):219, 1903.

[22] Hem C Kandpal, Gerhard H Fecher, and Claudia Felser. Calculated electronic and magnetic properties of the half-metallic, transition metal based heusler compounds. *Journal of Physics D: Applied Physics*, 40(6):1507, 2007.

[23] Zun-Yi Deng and Jian-Min Zhang. Half-metallic and magnetic properties of full-heusler alloys zr2crz (z= ga, in) with hg2cuti-type structure: A first-principles study. *Journal of Magnetism and Magnetic Materials*, 397:120–124, 2016.

[24] Erwin Schrödinger. An undulatory theory of the mechanics of atoms and molecules. *Physical review*, 28(6):1049, 1926.

[25] F Schwabl. Quantum mechanics (qm i). ; quantenmechanik (qm i). eine einfuehrung. 2007.

[26] Arthur Jabs. Connecting spin and statistics in quantum mechanics. *Foundations of Physics*, 40(7):776–792, 2010.

[27] Pierre Hohenberg and Walter Kohn. Inhomogeneous electron gas. *Physical review*, 136(3B):B864, 1964.

[28] DJ Griffiths. Introduction to quantum mechanics 2nd ed.-solutions. 2005.

[29] Max Born. Quantenmechanik der stoßvorgänge. *Zeitschrift für physik*, 38(11):803–827, 1926.

[30] David C Young. Density functional theory. *Computational Chemistry*, pages 42–48, 2001.

[31] Wolfgang Pauli. The connection between spin and statistics. *Physical Review*, 58(8):716, 1940.

[32] Nouredine Zettili. Quantum mechanics: concepts and applications, 2003.

[33] Klaus Capelle. A bird's-eye view of density-functional theory. *Brazilian journal of physics*, 36:1318–1343, 2006.

[34] Jean-Michel Combes, Pierre Duclos, and Ruedi Seiler. The born-oppenheimer approximation. In *Rigorous atomic and molecular physics*, pages 185–213. Springer, 1981.

[35] Niklas Zwettler. Density functional theory.

[36] Paul Adrien Maurice Dirac. A new notation for quantum mechanics. In *Mathematical Proceedings of the Cambridge Philosophical Society*, volume 35, pages 416–418. Cambridge University Press, 1939.

[37] A Szabo and NS Ostlund. Ch. 3. *Modern Quantum Chemistry: Introduction to Advanced Electronic Structure Theory*, 1989.

[38] Walter Kohn. Nobel lecture: Electronic structure of matter—wave functions and density functionals. *Reviews of Modern Physics*, 71(5):1253, 1999.

[39] Per-Olov Löwdin. Scaling problem, virial theorem, and connected relations in quantum mechanics. *Journal of Molecular Spectroscopy*, 3(1-6):46–66, 1959.

[40] M Turkyilmazoglu. Solution of the thomas–fermi equation with a convergent approach. *Communications in Nonlinear Science and Numerical Simulation*, 17(11):4097–4103, 2012.

[41] Andreas Görling. Density-functional theory beyond the hohenberg-kohn theorem. *Physical Review A*, 59(5):3359, 1999.

[42] Felix Brockherde, Leslie Vogt, Li Li, Mark E Tuckerman, Kieron Burke, and Klaus-Robert Müller. Bypassing the kohn-sham equations with machine learning. *Nature communications*, 8(1):1–10, 2017.

[43] Rüdiger Bauernschmitt and Reinhart Ahlrichs. Stability analysis for solutions of the closed shell kohn–sham equation. *The Journal of chemical physics*, 104(22):9047–9052, 1996.